

# Effect of columnar to equiaxed transition on microsegregation behaviour of main alloying elements in peritectic TiAl-based alloy

J. Lapin<sup>1\*</sup>, A. Klimová<sup>1,2</sup>, Z. Gabalcová<sup>1</sup>

<sup>1</sup>*Institute of Materials and Machine Mechanics, Slovak Academy of Sciences,  
Račianska 75, 831 02 Bratislava 3, Slovak Republic*

<sup>2</sup>*Institute of Materials Science, Faculty of Materials Science and Technology in Trnava,  
Slovak University of Technology in Bratislava, Paulínska 16, 917 24 Trnava, Slovak Republic*

Received 31 May 2013, received in revised form 19 June 2013, accepted 19 June 2013

## Abstract

The effect of columnar to equiaxed transition (CET) on the microsegregation behaviour of main alloying elements (Ti, Al and Nb) was studied in a peritectic Ti-44Al-5Nb-0.2B-0.2C (at.%) alloy. CET microstructures formed in cylindrical samples prepared by power down technique at a constant cooling rate of  $0.5 \text{ K s}^{-1}$  in a Bridgman type apparatus and in a large as-cast ingot were analysed. Microstructural analysis showed that the CET is not sharp but develops gradually during solidification in the studied alloy. A mixed zone composed of columnar and equiaxed grains is formed between the columnar and equiaxed zones. The size of columnar and equiaxed grains depends on the position in the as-cast cast ingot. The severity of the microsegregation expressed by segregation deviation parameters calculated for Nb decreases from columnar to the equiaxed zone in the samples prepared by power down technique as well as in the as-cast ingot. While the calculated segregation deviation parameters for Al and Ti decrease from columnar to equiaxed zone in the samples prepared by power down technique, these parameters show no evolution with the local microstructure in the as-cast ingot. The calculated values of segregation deviation parameters for Al and Ti are significantly lower than those for Nb in all analysed columnar, mixed and equiaxed zones of the samples.

**Key words:** titanium aluminides, TiAl, solidification, CET, energy-dispersive spectrometry, microsegregation

## 1. Introduction

Microstructure of large cast components from TiAl-based alloys usually consists of columnar grains growing from the mould surface and equiaxed grains formed in central zone of the castings [1–3]. Besides large anisotropy of mechanical properties resulting from such grain structure, columnar to equiaxed transition (CET) is also connected with formation of casting defects [1–4]. Various mechanisms and models have been proposed to explain CET during solidification of alloys [5–7]. There is a general consensus that the CET occurs when the moving front of columnar grains is blocked by equiaxed grains growing in the undercooled liquid ahead of this front, e.i., if the equiaxed grains are sufficient in size or number to arrest columnar grain growth.

Regardless of the blocking mechanisms, experiments and theoretical models have shown that the CET is significantly affected by the number of equiaxed grains and the nucleation undercooling. The CET is connected with a change of microsegregation severity of alloying elements. Martorano and Capocchi [8] and Doherty and Melford [9] reported for copper alloys and steels lower microsegregation severity in columnar dendrites than in equiaxed ones due to more extended homogenisation of the columnar structure. However, information about the effect of CET on microsegregation behaviour of alloying elements in TiAl-based alloys lacks in the literature. As shown by Klimová et al. [10], for directionally solidified (DS) peritectic Ti-44Al-5Nb-0.2B-0.2C (at.%) alloy with  $\beta$  (Ti-based solid solution with cubic crystal

\*Corresponding author: tel.: +421 2 49268290; fax: +421 2 49268312; e-mail address: [ummslapi@savba.sk](mailto:ummslapi@savba.sk)



Fig. 1. OM showing the typical macrostructure of longitudinal section of sample prepared by power down technique in Bridgman type apparatus: U – non-melted part, C<sub>1</sub> – columnar zone formed at a growth rate of  $V = 2.78 \times 10^{-4} \text{ m s}^{-1}$  and temperature gradient of  $G_L = 5.5 \times 10^3 \text{ K m}^{-1}$ , C<sub>2</sub> – columnar zone formed at a cooling rate of  $v = 0.5 \text{ K s}^{-1}$ , M – mixed columnar and equiaxed zone and E – equiaxed zone.

structure) primary solidification phase, severity of microsegregation decreases with increasing growth rate  $V$  in the mushy zone and only slightly increases below the mushy zone at the studied temperature gradients  $G_L$ . Except the zones located close to the dendrite tip, moderate decrease of segregation deviation parameter with the increase of temperature gradient was observed. As reported by Zollinger et al. [11] for Ti-46Al-8Nb (at.%) alloy prepared by quench during solidification technique [12], the microsegregation formed during solidification allows starting the solid phase transformation of the primary solidification  $\beta$  phase to  $\alpha$  phase (Ti-based solid solution with hexagonal crystal structure) at higher temperatures, and thus intensifies solid state segregation.

The aim of this paper is to study the effect of CET on microsegregation behaviour of main alloying elements (Ti, Al and Nb) in peritectic Ti-44Al-5Nb-0.2B-0.2C (at.%) alloy. Microsegregation behaviour is studied in two types of CET samples prepared: (i) at controlled solidification parameters in Bridgman type furnace using power down technique and (ii) by vacuum arc remelting and casting.

## 2. Experimental procedure

The intermetallic alloy with the nominal composition Ti-44Al-5Nb-0.2B-0.2C (at.%) and oxygen content of about 500 wtppm was supplied in the form of vacuum arc remelted conical ingot with a diameter changing from 35 to 60 mm and length of 310 mm. The ingot was cut to smaller blocks using electro spark machining, which were lathe machined to a diameter of 10 mm and length of 150 mm and put in dense cylindrical  $\text{Y}_2\text{O}_3$  moulds (purity of 99.5 %) with a diameter of 10/15 mm (inside/outside diameter) and length of 170 mm. Power down experiments were performed in a modified Bridgman type apparatus described elsewhere [13] under argon atmosphere. Before solidification, the vacuum chamber of the apparatus was evacuated to a pressure of 3 Pa, flushed with argon (purity 99.9995 %) six times, and then back-filled with argon at a pressure of 10 kPa, which was held constant during melting and solidification. The power down experiment consisted of: (i) heating of the

sample to a temperature of 1993 K at a heating rate of  $0.355 \text{ K s}^{-1}$ , (ii) stabilisation at the temperature of 1993 K for 300 s, (iii) partial displacement of the sample from the hot zone of the furnace into the crystalliser at a constant growth rate of  $2.78 \times 10^{-4} \text{ m s}^{-1}$  to a length of 20 mm, (iv) temperature decrease from 1993 to 1693 K at constant cooling rate of  $0.5 \text{ K s}^{-1}$  and (v) furnace cooling of the sample from 1693 K to room temperature.

Microstructural investigations were performed by optical microscopy (OM) and backscattered scanning electron microscopy (BSEM). Chemical composition and distribution of main alloying elements were measured by energy-dispersive X-ray spectroscopy (EDS). OM, SEM and EDS samples were prepared using standard grinding and polishing metallographic techniques. The samples for optical microscopy were chemically etched in a reagent of 100 ml  $\text{H}_2\text{O}$ , 10 ml  $\text{HNO}_3$  and 3 ml HF. JEOL JSM-7600F ultrahigh resolution field emission scanning electron microscope with detector for backscattered electrons (BSEM) was used for the observations of the microstructure of the studied alloy in SEM, and COMPO mode with acceleration voltage 10 and 15 kV. EDS area and point analyses along a line were carried out after quant optimisation on Ti and calibration on standard with nominal composition Ti-46Al-8Nb (at.%). The preparation of homogeneous standards for calibration of EDS equipment was described elsewhere [14].

## 3. Results

### 3.1. CET in samples prepared by power down technique

Figure 1 shows the typical macrostructure of the samples prepared by power down technique in Bridgman type apparatus. The macrostructure consists of five different zones designated as U, C<sub>1</sub>, C<sub>2</sub>, M and E. The zone designated as U with an average length of 12 mm represents the non-melted part of the sample composed of equiaxed grains. The zone C<sub>1</sub> with an average length of 20 mm is composed of columnar grains which were formed by directional solidification at a constant growth rate of  $V = 2.78 \times 10^{-4}$

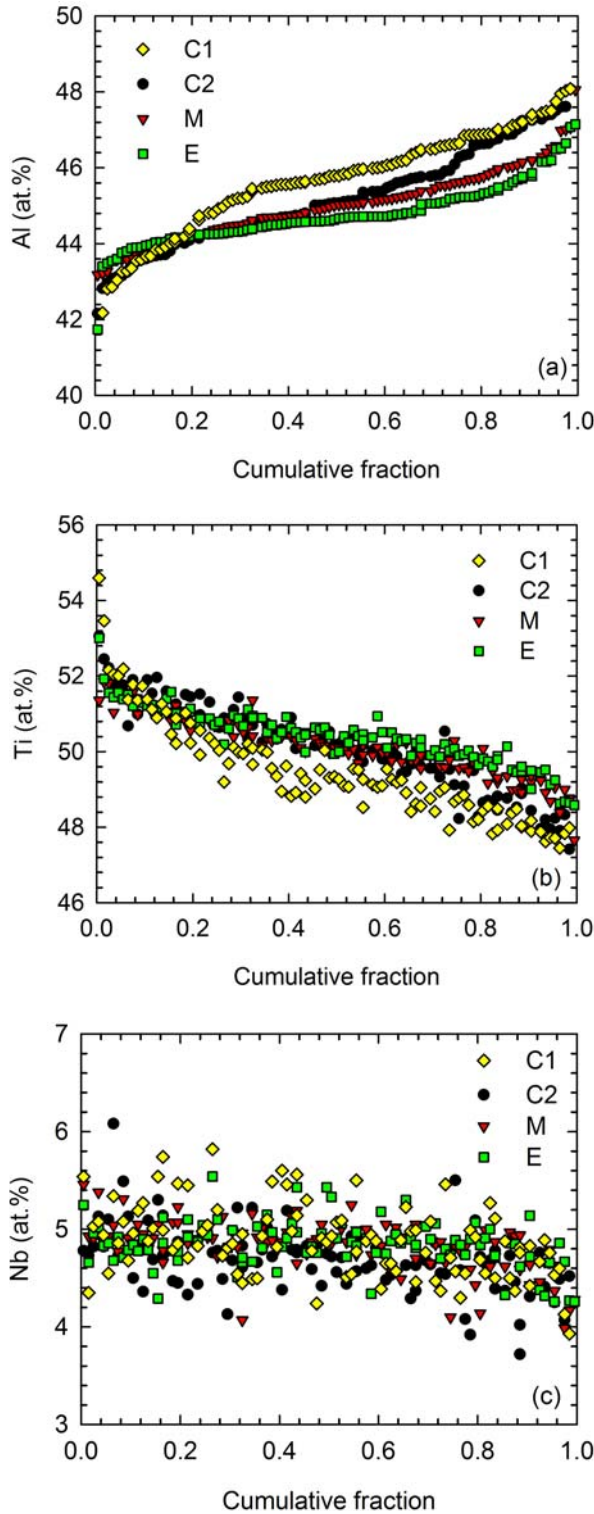


Fig. 2. Evolution of concentration of main alloying elements with cumulative fraction of solid in columnar (C1, C2), mixed (M) and equiaxed (E) zones of the sample prepared by power down technique: (a) Al, (b) Ti and (c) Nb.

$\text{m s}^{-1}$  and constant temperature gradient in liquid at the solid liquid interface of  $G_L = 5.5 \times 10^3 \text{ K m}^{-1}$ .

The zone C2 represents columnar grain structure with an average length of 35 mm, which was formed by power down technique at a constant cooling rate of  $0.5 \text{ K s}^{-1}$ . Different solidification parameters for the grain growth in the zones C1 and C2 lead to two different average diameters of the columnar grains of 2.0 and 4.0 mm, respectively. The mixed zone M with an average length of 25 mm represents microstructure composed of columnar and equiaxed grains. In this zone, the equiaxed grains are distributed preferentially between the columnar grains. The equiaxed zone E contains relatively large equiaxed grains with an average diameter of 4.0 mm.

Microsegregation behaviour of the main alloying elements in the samples prepared by power down technique was investigated on the longitudinal sections in the zones C1, C2, M and E. Data from EDS measurements were sorted using single-element sorting scheme with Al as the main sorting element [15]. Cumulative fraction  $f(i)$  was assigned to each measured point  $i$ . Since absolute maximum and minimum concentrations cannot be guaranteed for the sample using random sampling, cumulative fraction was assigned to [15]:

$$f(i) = (R_i - 0.5)/N, \quad (1)$$

where  $R_i$  is the rank number and  $N$  is the total number of points. Hence,  $f(i)$  continuously varies from 0 to 1 ( $0 < f(i) < 1$ ). Figure 2 shows dependence of concentration of Al, Ti and Nb on cumulative fraction of solid in the analysed zones C1, C2, M and E. Each EDS profile consists of 100 individual measurements. The concentration profiles in the zone E reflect intensive homogenisation of the alloy (Figs. 2a,b,c), which is caused by transformation of columnar grain structure to equiaxed one and solid phase transformations during cooling. For quantitative evaluation of severity of microsegregation, segregation deviation parameter  $\sigma_m^j$  was calculated for each alloying element  $j$  in the zones C1, C2, M and E according to relationship [8, 16]:

$$\sigma_m^j = \frac{1}{NC_0^j} \sum_{i=1}^N |C_i^j - C_0^j|, \quad (2)$$

where  $C_0^j$  is the average concentration of the  $j$ th element,  $C_i^j$  is the concentration of the  $j$ th element at the point  $i$  and  $N$  is the total number of the analysed points for one analysed zone. Figure 3 shows the variations of segregation deviation parameters  $\sigma_m^{\text{Al}}$  for Al,  $\sigma_m^{\text{Ti}}$  for Ti and  $\sigma_m^{\text{Nb}}$  for Nb with the analysed zones C1, C2, M and E. It should be noted that the calculated segregation deviation parameter is the highest one for Nb in the zone C1 and decreases towards the zone E. The segregation deviation parameters for Al and Ti



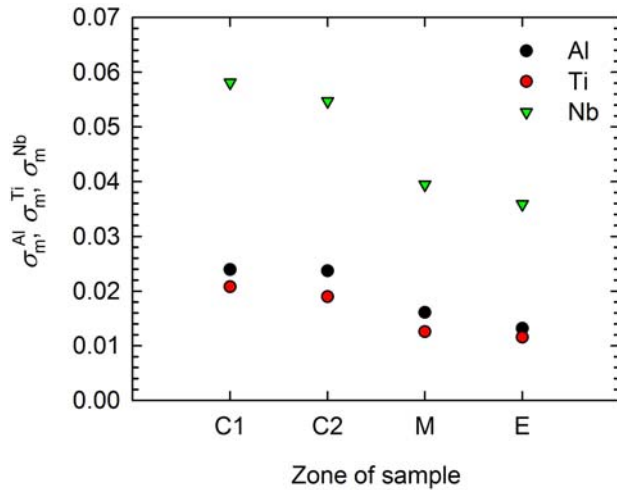


Fig. 3. Variation of the segregation deviation parameter  $\sigma_m^{Al}$  for Al,  $\sigma_m^{Ti}$  for Ti and  $\sigma_m^{Nb}$  for Nb with the columnar (C1 and C2), mixed (M) and equiaxed (E) zone in the sample prepared by power down technique.

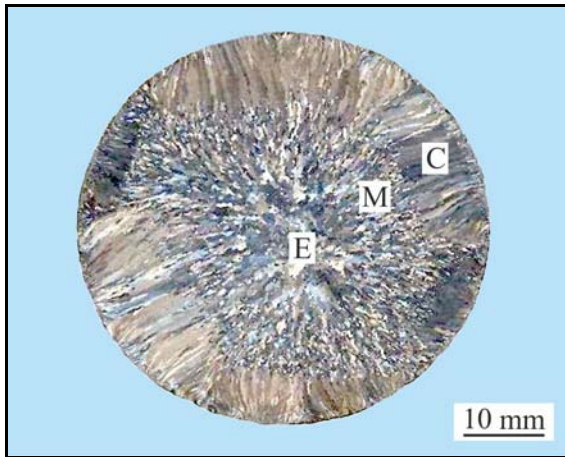


Fig. 4. OM showing the typical macrostructure on transversal section of the bottom part (BP) of the as-cast ingot: C – columnar zone, M – mixed columnar and equiaxed zone, and E – equiaxed zone.

are significantly lower than those for Nb and decrease from the zone C1 towards the zone E.

### 3.2 CET in as-cast ingot

Figure 4 shows the typical macrostructure observed on investigated transversal sections of the as-cast ingot. Three zones with different type of microstructure designated as C, M and E can be well distinguished. Thin chill zone composed of fine equiaxed grains in the vicinity of the surface of the ingot is followed by columnar grain zone C. The mixed zone (M) is composed of columnar and equiaxed grains. The CET is complete in the central equiaxed zone (E) of

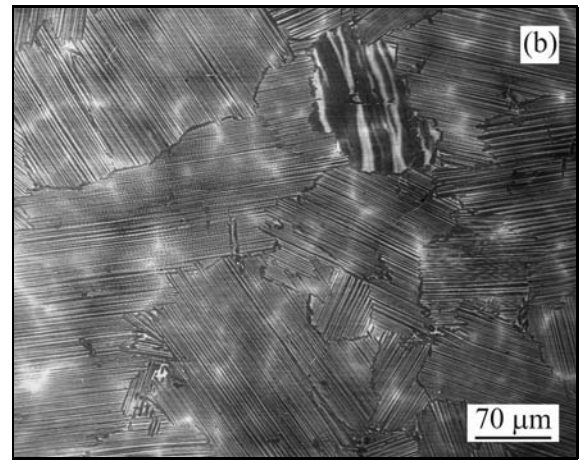
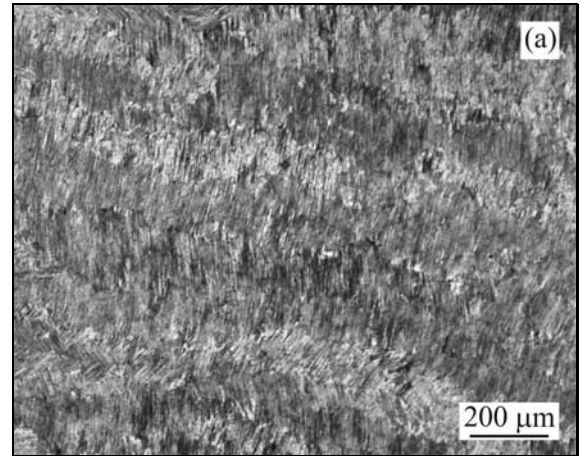


Fig. 5. Morphology of grains in the as-cast ingot: (a) columnar grains, OM; (b) equiaxed grains, BSEM.

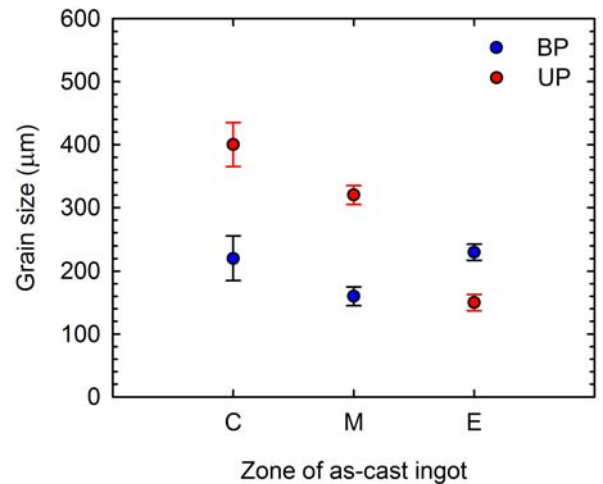


Fig. 6. Variation of grain size with columnar C, mixed M and equiaxed E zone of the as-cast ingot. BP – bottom part of the ingot; UP – upper part of the ingot.

the ingot. The typical morphology of columnar and equiaxed grains is shown in Fig. 5. Figure 6 shows

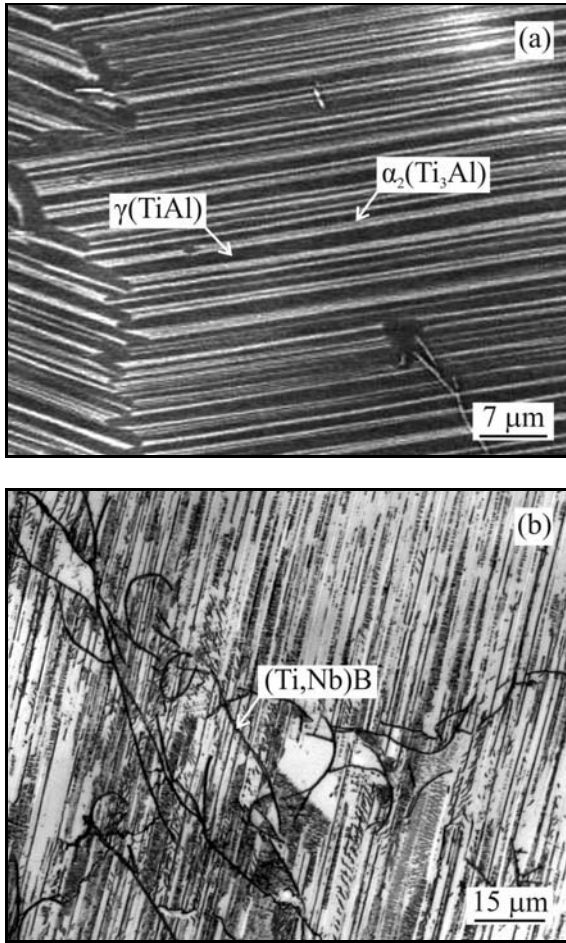


Fig. 7. Microstructure of the as-cast ingot: (a) lamellar  $\alpha_2 + \gamma$  microstructure of columnar and equiaxed grains, BSEM; (b) ribbon-like (Ti, Nb)B particles in the interdendritic region, OM.

variation of grain size within the zones C, M and E. In the bottom part (BP) of the ingot, an average diameter of columnar grains of 220  $\mu\text{m}$  within the zone C abruptly decreases to 160  $\mu\text{m}$  in the zone M. The central zone E contains equiaxed grains with the average diameter of 230  $\mu\text{m}$ . In the upper part (UP) of the ingot, the average diameter of columnar grains is 400  $\mu\text{m}$  in the zone C and decreases to 320  $\mu\text{m}$  in the zone M. The zone E contains grains with the average size of 150  $\mu\text{m}$ . The average diameter of central equiaxed grain zone is measured to be 10 and 15 mm in the BP and UP of the ingot, respectively. According to EDS and XRD analyses [10, 17], the lamellar microstructure of the columnar and equiaxed grains is formed by  $\alpha_2(\text{Ti}_3\text{Al})$  and  $\gamma(\text{TiAl})$  phases (Fig. 7a). In some regions of the ingot, coarse equiaxed  $\alpha_2$  and  $\beta/\text{B2}$  (disordered/ordered Ti-based solid solution with cubic crystal structure) particles occur in the microstructure. The occurrence of B2 particles mostly within the dendrites is associated with the ordering of the residual primary  $\beta$ -phase [18]. In addition, the studied

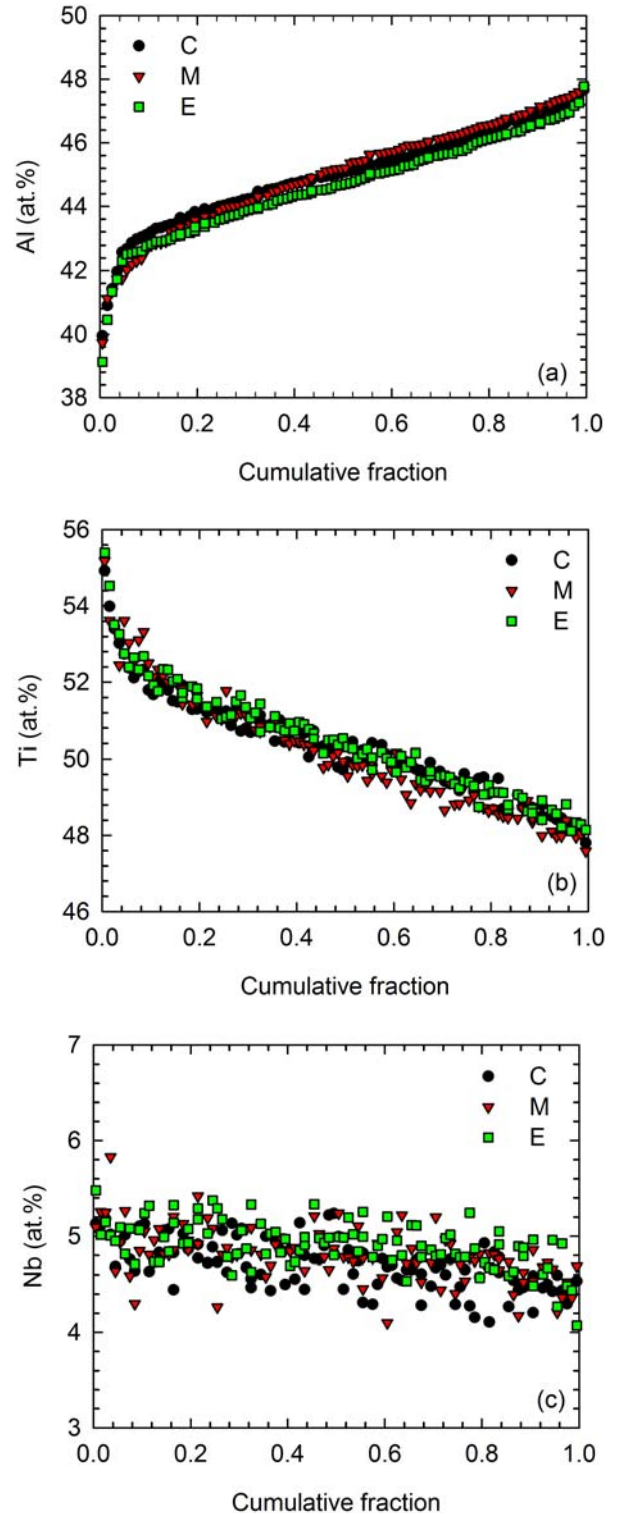


Fig. 8. Evolution of concentration of main alloying elements with cumulative fraction of solid in columnar (C), mixed (M) and equiaxed (E) zone in the bottom part (BP) of the as-cast ingot: (a) Al, (b) Ti and (c) Nb.

alloy contains ribbon-like boride particles, which are preferentially formed within the interdendritic region during the solidification of the last liquid, as shown

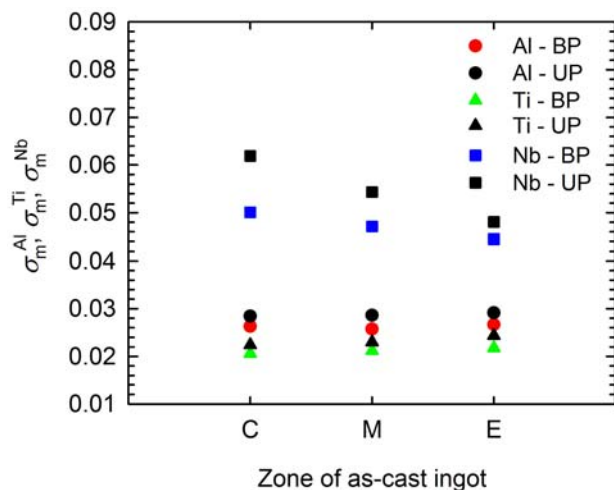


Fig. 9. Variation of the segregation deviation parameters  $\sigma_m^{\text{Al}}$  for Al,  $\sigma_m^{\text{Ti}}$  for Ti and  $\sigma_m^{\text{Nb}}$  for Nb with the columnar (C), mixed (M) and equiaxed (E) zone in the as-cast ingot. BP – bottom part of the ingot; UP – upper part of the ingot.

in Fig. 7b. According to Kitkamthorn et al. [19], four types of borides can be formed in the TiAl-based systems alloyed with Nb and B: (i) TiB with B<sub>27</sub>, (Ti, Nb)B with B<sub>f</sub>, Ti<sub>3</sub>B<sub>4</sub> with orthorhombic and TiB<sub>2</sub> with hexagonal crystal structures. The XRD analysis of the studied alloy showed only the presence of (Ti, Nb)B borides with metastable *oC8* (B<sub>f</sub>) crystal structure [10], what is in agreement with the results reported recently by Hecht et al. [20].

Figure 8 shows dependence of concentration of Al, Ti and Nb on cumulative fraction of solid in the columnar (C), mixed (M) and equiaxed (E) zones of the BP of the ingot (see Fig. 4). The EDS profiles consist of 100 individual measurements. The concentration profiles of the individual elements do not indicate clear differences among the analysed zones, as seen in Figs. 8a,b,c. Figure 9 shows variations of the segregation deviation parameters  $\sigma_m^{\text{Al}}$  for Al,  $\sigma_m^{\text{Ti}}$  for Ti and  $\sigma_m^{\text{Nb}}$  for Nb with the analysed zones C, M and E for the BP and UP of the ingot. It is worth noting that the segregation deviation parameter is the highest one for Nb in the zone C and decreases towards the equiaxed zone E in both parts of the ingot. The segregation deviation parameters  $\sigma_m^{\text{Al}}$  and  $\sigma_m^{\text{Ti}}$  are significantly lower than those of  $\sigma_m^{\text{Nb}}$  and their variation with the analysed microstructural zones is negligible for both parts of the ingot.

## 4. Discussion

### 4.1. Mechanisms of CET

The observed CET is not sharp in the studied alloy and the mixed zone composed of columnar and

equiaxed grains is formed in the samples prepared by power down technique as well as in the as-cast ingot (Figs. 1 and 4). Such a type of mixed columnar-equiaxed grain zone was also observed by Ares et al. [21–23] in Al-Cu, Zn-Al and Pb-Sn alloys. Pineda and Martorano [24] showed that gradual addition of Al-Ti-B inoculant led to a gradual increase in the number of equiaxed grains coexisting with columnar grains in the mixed zone of Al-Si alloys. Lapin and Gabalová [4] observed sharp interface between columnar and equiaxed grains in Ti-46Al-8Nb (at.%) alloy prepared at non-steady state growth conditions characterised by continuous change of the growth rate and temperature gradient in a Bridgman type apparatus. Gandin [25] and Martorano et al. [6] found sharp interface between columnar and equiaxed grains in Al-Si systems using multiphase/multiscale model based on mechanical blocking and solutal interaction between equiaxed grains and advancing columnar front.

To obtain CET, the following is required: (i) the presence of undercooled liquid ahead or near the columnar front in which equiaxed grains nucleate and grow and (ii) equiaxed grains of sufficient size and/or number beside/attached to the columnar interface to arrest the columnar growth [26]. In the samples prepared by the power down technique, the CET is favoured by high growth rate  $V$  and low temperature gradient  $G_L$  [26]. Martorano et al. [6] proposed a mechanism for the CET based on solutal interactions between the equiaxed grains and the advancing columnar front. The solute blocking is achieved by the undercooling that drives dendrite tip growth on the average solute concentration of the liquid surrounding the grain envelopes instead of the initial alloy composition. Newly nucleated grains can fall down either on the columnar dendrite or towards the liquid area. Hence, sides of the columnar dendrite can be gradually filled in with equiaxed dendrites. Therefore, a post-mortem analysis of the samples could lead to the false conclusion that the structure is mixed columnar-equiaxed, whereas it is only caused by sedimentation [28].

In small as-cast ingots, a large number of equiaxed grain nuclei may be formed near the mould wall at the time of pouring, owing to thermal undercooling and growth restriction of the grains caused by solute redistribution [26]. Because of the high density of rapidly growing equiaxed grains that may exist throughout the liquid, the CET will be sharp and occur over a large part of the columnar front at the same time. In the studied as-cast ingot, it is unlikely that the equiaxed grains originating at the mould walls are sufficient to arrest columnar growth, and other mechanisms such as dendrite fragmentation are important [26]. The CET occurs gradually over the advancing columnar front probably due to equiaxed grains settling onto the lower part of the front or attachment of



individual grains to the vertical faces. An insufficient fraction of grains reaching/attaching to the front leads to entrapment of the equiaxed grains in the columnar zone and formation of the mixed zone.

#### 4.2. Effect of local solidification parameters on microsegregation

As shown recently by Klimová et al. [10, 29] for DS Ti-44Al-5Nb-0.2B-0.2C (at.%) alloy, segregation deviation parameters slightly increase with increasing growth rate  $V$  and decrease with increasing temperature gradient  $G_L$  below the mushy zone of the quench during solidification samples. As shown in Fig. 3, the segregation deviation parameters for the main alloying elements decrease from the columnar zone C1 towards the equiaxed zone E. The columnar zone C1 results from the directional solidification at the constant growth rate of  $V = 2.78 \times 10^{-4} \text{ m s}^{-1}$  and constant temperature gradient of  $G_L = 5.5 \times 10^3 \text{ K m}^{-1}$ . In this zone, the highest measured segregation deviation parameters of the main alloying elements result mainly from the high  $V$ , the effect of which is reduced only partially by high  $G_L$ . As shown by numerical calculations based on experimental measurements of temperature distribution during power down solidification by Mooney et al. [30], the local solidification conditions in the columnar zone C2 and mixed zone M can be characterised by a continuous increase of  $V$  from about  $5 \times 10^{-6}$  to about  $1 \times 10^{-4} \text{ m s}^{-1}$  and decrease of  $G_L$  from about  $5 \times 10^3$  to about  $7 \times 10^2 \text{ K m}^{-1}$ . The lower  $V$  calculated for the zones C2 and M than that in the zone C1 should lead to a decrease of segregation deviation parameters, which can be compensated by decreasing  $G_L$  only partially. The local combinations of  $V$  and  $G_L$  favour continuous decrease of the segregation deviation parameters in the columnar zone C2 and mixed zone M, as shown in Fig. 3. The equiaxed microstructure in the zone E, which is formed at the lowest  $G_L$ , is characterised by the lowest values of the segregation deviation parameters. Previous works on Al-Si alloys [27, 31] using power down technique showed that the equiaxed zone was formed at a critical undercooling of 5 K. It should be noted that the calculated segregation deviation parameters for the studied alloy are affected by the solid phase transformations during cooling. Lower cooling rates result in more complete transformation of the primary  $\beta$  phase and more extended homogenisation of the forming  $\alpha$  phase due to longer soaking time in the single  $\alpha$  phase field. Hence, redistribution of the alloying elements in the power down samples passing complete temperature profile of the furnace can be significantly affected by the solid state homogenisation processes during cooling and may deviate from the findings reported recently by Klimová et al. [10, 29] for the samples pre-

pared by quench during directional solidification technique.

The local solidification conditions affecting redistribution of alloying elements are more complex in the as-cast ingot. The highest local values of  $V$  and  $G_L$  are in the vicinity of the surface and decrease towards the central region of the ingot. However, since the ingot was prepared by a vacuum casting, some fluctuations in thermal conditions could affect redistribution of the alloying elements, origin of which cannot be assessed fully by post-mortem analysis of the microstructure [8]. The decrease of segregation deviation parameter for Nb from columnar to equiaxed zone corresponds very well to its evolution in the samples prepared by power down technique. On the contrary to the power down samples, the calculated values of  $\sigma_m^{\text{Al}}$  and  $\sigma_m^{\text{Ti}}$  are not significantly affected by the local type of microstructure in both parts of the ingot.

## 5. Conclusions

The investigation of the effect of columnar to equiaxed transition on the microsegregation behaviour of main alloying elements in a peritectic Ti-44Al-5Nb-0.2B-0.2C (at.%) alloy can be summarised as follows:

1. The CET is not sharp but develops gradually during solidification of the studied alloy. The mixed zone composed of columnar and equiaxed grains is formed between the columnar and equiaxed zones in the samples prepared by power down technique as well as in the as-cast ingot. The size of columnar and equiaxed grains depends on the position in the as-cast cast ingot.

2. The severity of the microsegregation expressed by segregation deviation parameters calculated for Al, Ti and Nb decreases from the columnar zone to the equiaxed zone in the samples prepared by power down technique. The calculated segregation deviation parameters for Al and Ti are significantly lower than that for Nb. The evolution of the segregation deviation parameters within the samples can be attributed to local variations of solidification parameters.

3. The segregation deviation parameter for Nb decreases from the columnar to equiaxed zone in the as-cast ingot. The segregation deviation parameters for Al and Ti are significantly lower than that for Nb and show negligible variations with the local microstructure.

## Acknowledgements

This work is based on the results of the project Competence center for new materials, advanced technologies and energy ITMS 26240220073, supported by the Research and Development Operational Program funded by the European Regional Development Fund.

## References

- [1] Lapin, J., Nazmy, M.: *Mater. Sci. Eng. A*, 380, 2004, p. 298. [doi:10.1016/j.msea.2004.05.011](https://doi.org/10.1016/j.msea.2004.05.011)
- [2] Lapin, J., Frkáňová, K.: *Kovove Mater.*, 49, 2011, p. 243.
- [3] Lapin, J.: In: *Technológia 2011*. Bratislava, STU 2011, p. 3.
- [4] Lapin, J., Gabalcová, Z.: *Intermetallics*, 19, 2011, p. 797. [doi:10.1016/j.intermet.2010.11.021](https://doi.org/10.1016/j.intermet.2010.11.021)
- [5] Hunt, J. D.: *Mater. Sci. Eng.*, 65, 1984, p. 75. [doi:10.1016/0025-5416\(84\)90201-5](https://doi.org/10.1016/0025-5416(84)90201-5)
- [6] Martorano, M. A., Beckermann, C., Gandin, C. A.: *Metall. Mater. Trans. A*, 34A, 2003, p. 1657. [doi:10.1007/s11661-003-0311-x](https://doi.org/10.1007/s11661-003-0311-x)
- [7] Biscuola, V. B., Martorano, M. A.: *Metall. Mater. Trans. A*, 39A, 2008, p. 2885. [doi:10.1007/s11661-008-9643-x](https://doi.org/10.1007/s11661-008-9643-x)
- [8] Martorano, M. A., Capocchi, J. D. T.: *Metall. Mater. Trans. A*, 31A, 2000, p. 3137. [doi:10.1007/s11661-000-0093-3](https://doi.org/10.1007/s11661-000-0093-3)
- [9] Doherty, M. D., Melford, D. A.: *J. Iron Steel Inst.*, 204, 1966, p. 1131.
- [10] Klimová, A., Lapin, J., Pelachová, T., Nosko, M.: *Kovove Mater.*, 51, 2013, p. 89.
- [11] Zollinger, J., Gabalcová, Z., Daloz, D., Lapin, J., Combeau, H.: *Kovove Mater.*, 46, 2008, p. 291.
- [12] Gabalcová, Z., Lapin, J.: *Kovove Mater.*, 45, 2007, p. 231.
- [13] Lapin, J., Ondrůš, L., Nazmy, M.: *Intermetallics*, 10, 2002, p. 1019. [doi:10.1016/S0966-9795\(02\)00119-X](https://doi.org/10.1016/S0966-9795(02)00119-X)
- [14] Klimová, A.: In: *7th Seminar of Central European PhD Students – Research in Materials Science*, 2012, Trnava.
- [15] Ganesan, M., Dye, D., Lee, P. D.: *Metall. Mater. Trans. A*, 36A, 2005, p. 2191. [doi:10.1007/s11661-005-0338-2](https://doi.org/10.1007/s11661-005-0338-2)
- [16] Charpentier, M., Daloz, D., Gautier, E., Lesoult, G., Hazotte, A., Grange, M.: *Metall. Mater. Trans. A*, 34A, 2003, p. 2139. [doi:10.1007/s11661-003-0278-7](https://doi.org/10.1007/s11661-003-0278-7)
- [17] Klimová, A., Lapin, J.: In: *Conference METAL 2012 Proceedings: 21st International Conference on Metallurgy and Materials*. Brno 2012. ISBN 978-80-87294-29-1. PMCid:3170738.
- [18] Daloz, D., Hecht, U., Zollinger, J., Combeau, H., Hazotte, A., Zaloznik, M.: *Intermetallics*, 19, 2010, p. 749. [doi:10.1016/j.intermet.2010.11.013](https://doi.org/10.1016/j.intermet.2010.11.013)
- [19] Kitkamthorn, U., Zhang, L. C., Aindow, M.: *Intermetallics*, 14, 2006, p. 759. [doi:10.1016/j.intermet.2005.11.013](https://doi.org/10.1016/j.intermet.2005.11.013)
- [20] Hecht, U., Witusiewicz, V., Drevermann, A., Zollinger, J.: *Intermetallics*, 16, 2008, p. 969. [doi:10.1016/j.intermet.2008.04.019](https://doi.org/10.1016/j.intermet.2008.04.019)
- [21] Ares, A. E., Gueijman, S. F., Schveyov, C. E.: *J. Crystal Growth*, 312, 2010, p. 2154. [doi:10.1016/j.jcrysgro.2010.04.040](https://doi.org/10.1016/j.jcrysgro.2010.04.040)
- [22] Ares, A. E., Schveyov, C. E.: *Metall. Mater. Trans. A*, 38A, 2007, p. 1485. [doi:10.1007/s11661-007-9111-z](https://doi.org/10.1007/s11661-007-9111-z)
- [23] Ares, A. E., Schveyov, C. E.: *Metall. Mater. Trans. A*, 31A, 2000, p. 1611. [doi:10.1007/s11661-000-0171-6](https://doi.org/10.1007/s11661-000-0171-6)
- [24] Pineda, D. A., Martorano, M. A.: *Acta Mater.*, 61, 2013, p. 1785. [doi:10.1016/j.actamat.2012.12.002](https://doi.org/10.1016/j.actamat.2012.12.002)
- [25] Gandin, C.-A.: *ISIJ International*, 40, 2000, p. 971.
- [26] Spittle, J. A.: *International Materials Reviews*, 51, 2006, p. 247. [doi:10.1179/174328006X102493](https://doi.org/10.1179/174328006X102493)
- [27] Sturz, L., Drevermann, A., Pickmann, C., Zimmermann, G.: *Mater. Sci. Eng. A*, 413–414, 2005, p. 379. [doi:10.1016/j.msea.2005.08.199](https://doi.org/10.1016/j.msea.2005.08.199)
- [28] Reinhart, G., Mangelinck-Noel, N., Nguyen-Thi, H., Schenk, T., Gastaldi, J., Billia, B., Pino, P., Hartwig, J., Baruchel, J.: *Mater. Sci. Eng. A*, 413–414, 2005, p. 384. [doi:10.1016/j.msea.2005.08.197](https://doi.org/10.1016/j.msea.2005.08.197)
- [29] Klimová, A., Gabalcová, Z., Lapin, J.: In: *Conference METAL 2013 Proceedings: 22nd International Conference on Metallurgy and Materials*. Brno, Tanger 2013. ISBN 978-80-87294-39-0.
- [30] Mooney, R., McFadden, S., Lapin, J., Gabalcová, Z.: in preparation.
- [31] McFadden, S., Browne, D. J., Gandin, C.-A.: *Metall. Mater. Trans. A*, 40A, 2009, p. 662. [doi:10.1007/s11661-008-9708-x](https://doi.org/10.1007/s11661-008-9708-x)